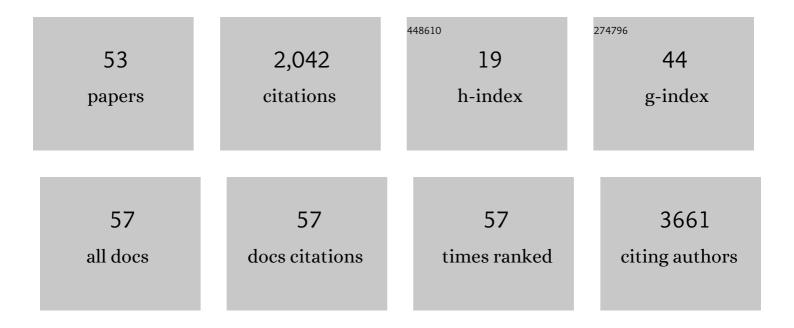
## Yann Seimbille

List of Publications by Year in descending order

Source: https://exaly.com/author-pdf/7054532/publications.pdf Version: 2024-02-01



YANN SEIMBILLE

#	Article	IF	CITATIONS
1	Towards Complete Tumor Resection: Novel Dual-Modality Probes for Improved Image-Guided Surgery of GRPR-Expressing Prostate Cancer. Pharmaceutics, 2022, 14, 195.	2.0	6
2	Improved Multimodal Tumor Necrosis Imaging with IRDye800CW-DOTA Conjugated to an Albumin-Binding Domain. Cancers, 2022, 14, 861.	1.7	0
3	New Developments in Carbonic Anhydrase IX-Targeted Fluorescence and Nuclear Imaging Agents. International Journal of Molecular Sciences, 2022, 23, 6125.	1.8	5
4	Pharmacological evaluation of imidazoleâ€derived bisphosphonates on receptor activator of nuclear factorâ€îºB ligandâ€induced osteoclast differentiation and function. Chemical Biology and Drug Design, 2021, 97, 121-133.	1.5	3
5	Cancer-Associated Fibroblasts as Players in Cancer Development and Progression and Their Role in Targeted Radionuclide Imaging and Therapy. Cancers, 2021, 13, 1100.	1.7	35
6	Development of [225Ac]Ac-PSMA-I&T for Targeted Alpha Therapy According to GMP Guidelines for Treatment of mCRPC. Pharmaceutics, 2021, 13, 715.	2.0	28
7	Necrosis binding of Ac-Lys0(IRDye800CW)-Tyr3-octreotate: a consequence from cyanine-labeling of small molecules. EJNMMI Research, 2021, 11, 47.	1.1	5
8	IEDDA: An Attractive Bioorthogonal Reaction for Biomedical Applications. Molecules, 2021, 26, 4640.	1.7	28
9	EANM guideline for harmonisation on molar activity or specific activity of radiopharmaceuticals: impact on safety and imaging quality. EJNMMI Radiopharmacy and Chemistry, 2021, 6, 34.	1.8	26
10	Tumor Microenvironment Responsive "Head-to-Foot―Self-Assembly Nanoplatform for Positron Emission Tomography Imaging in Living Subjects. ACS Nano, 2021, 15, 18250-18259.	7.3	12
11	In Vivo Evaluation of Gallium-68-Labeled IRDye800CW as a Necrosis Avid Contrast Agent in Solid Tumors. Contrast Media and Molecular Imaging, 2021, 2021, 1-8.	0.4	3
12	A novel clickable MSAP agent for dual fluorescence/nuclear labeling of biovectors. Organic and Biomolecular Chemistry, 2020, 18, 6134-6139.	1.5	4
13	Radiofluorinated Smart Probes for Noninvasive PET Imaging of Legumain Activity in Living Subjects. Analytical Chemistry, 2020, 92, 11627-11634.	3.2	12
14	Higher availability of α4β2 nicotinic receptors (nAChRs) in dorsal ACC is linked to more efficient interference control. NeuroImage, 2020, 214, 116729.	2.1	6
15	In Vivo Evaluation of Indium-111–Labeled 800CW as a Necrosis-Avid Contrast Agent. Molecular Imaging and Biology, 2020, 22, 1333-1341.	1.3	6
16	Therapeutic Applications of Pretargeting. Pharmaceutics, 2019, 11, 434.	2.0	38
17	Rational design of caspase-responsive smart molecular probe for positron emission tomography imaging of drug-induced apoptosis. Theranostics, 2019, 9, 6962-6975.	4.6	24
18	A Flexible Synthesis of 68Ga-Labeled Carbonic Anhydrase IX (CAIX)-Targeted Molecules via CBT/1,2-Aminothiol Click Reaction. Molecules, 2019, 24, 23.	1.7	27

YANN SEIMBILLE

#	Article	lF	CITATIONS
19	Nicotinic receptor abnormalities as a biomarker in idiopathic generalized epilepsy. European Journal of Nuclear Medicine and Molecular Imaging, 2019, 46, 385-395.	3.3	14
20	Early‣tage Incorporation Strategy for Regioselective Labeling of Peptides using the 2 yanobenzothiazole/1,2â€Aminothiol Bioorthogonal Click Reaction. ChemistryOpen, 2018, 7, 256-261.	0.9	11
21	Early-Stage Incorporation Strategy for Regioselective Labeling of Peptides using the 2-Cyanobenzothiazole/ 1,2-Aminothiol Bioorthogonal Click Reaction. ChemistryOpen, 2018, 7, 214-214.	0.9	0
22	Two bifunctional desferrioxamine chelators for bioorthogonal labeling of biovectors with zirconium-89. Organic and Biomolecular Chemistry, 2018, 16, 5102-5106.	1.5	8
23	Long-term Results of a Comparative PET/CT and PET/MRI Study of 11C-Acetate and 18F-Fluorocholine for Restaging of Early Recurrent Prostate Cancer. Clinical Nuclear Medicine, 2017, 42, e242-e246.	0.7	15
24	Preclinical validations of [18F]FPyPEGCBT-c(RGDfK): a 18F-labelled RGD peptide prepared by ligation of 2-cyanobenzothiazole and 1,2-aminothiol to image angiogenesis. EJNMMI Radiopharmacy and Chemistry, 2017, 1, 16.	1.8	5
25	[ \$\${}^{11}hbox {C}\$\$ 11 C ]acetate and PET/CT assessment of muscle activation in rat studies. International Journal of Computer Assisted Radiology and Surgery, 2016, 11, 733-743.	1.7	0
26	Role of MIF/CD74 signaling pathway in the development of pleural mesothelioma. Oncotarget, 2016, 7, 11512-11525.	0.8	10
27	A novel 2-cyanobenzothiazole-based 18F prosthetic group for conjugation to 1,2-aminothiol-bearing targeting vectors. Organic and Biomolecular Chemistry, 2015, 13, 3667-3676.	1.5	19
28	Study of rat skeletal muscle activation by PET/CT and [ <sup>11</sup> C]acetate. , 2015, , .		0
29	Gut Microbiota Orchestrates Energy Homeostasis during Cold. Cell, 2015, 163, 1360-1374.	13.5	581
30	Microbiota depletion promotes browning of white adipose tissue and reduces obesity. Nature Medicine, 2015, 21, 1497-1501.	15.2	324
31	PET Molecular Imaging of Hypoxia in Ischemic Stroke: An Update. Current Vascular Pharmacology, 2015, 13, 209-217.	0.8	12
32	First imaging results of an intraindividual comparison of 11C-acetate and 18F-fluorocholine PET/CT in patients with prostate cancer at early biochemical first or second relapse after prostatectomy or radiotherapy. European Journal of Nuclear Medicine and Molecular Imaging, 2014, 41, 68-78.	3.3	46
33	Synthesis of a nonâ€peptidic PET tracer designed for <i>α</i> <sub>5</sub> <i>β</i> <sub>1</sub> integrin receptor. Journal of Labelled Compounds and Radiopharmaceuticals, 2014, 57, 365-370.	0.5	2
34	Study of skeletal muscle behavior by PET/MRI. , 2014, , .		2
35	PET Radiotracers for Molecular Imaging in Dementia. Current Radiopharmaceuticals, 2014, 6, 215-230.	0.3	8
36	Synthesis and in vitro evaluation of a novel radioligand for αvβ3 integrin receptor imaging: [18F]FPPA-c(RGDfK). Bioorganic and Medicinal Chemistry Letters, 2013, 23, 6068-6072.	1.0	7

YANN SEIMBILLE

#	Article	IF	CITATIONS
37	Matching between regional coronary vasodilator capacity and corresponding circumferential strain in individuals with normal and increasing body weight. Journal of Nuclear Cardiology, 2012, 19, 693-703.	1.4	4
38	[11C]acetate PET/CT Visualizes Skeletal Muscle Exercise Participation, Impaired Function, and Recovery after Hip Arthroplasty; First Results. Molecular Imaging and Biology, 2011, 13, 793-799.	1.3	6
39	Elevated endocannabinoid plasma levels are associated with coronary circulatory dysfunction in obesity. European Heart Journal, 2011, 32, 1369-1378.	1.0	123
40	Structural epicardial disease and microvascular function are determinants of an abnormal longitudinal myocardial blood flow difference in cardiovascular risk individuals as determined with PET/CT. Journal of Nuclear Cardiology, 2010, 17, 1023-1033.	1.4	28
41	Combined evaluation of myocardial perfusion and coronary morphology in the identification of subclinical CAD. Nuklearmedizin - NuclearMedicine, 2010, 49, 173-182.	0.3	3
42	High efficiency production and purification of 86Y based on electrochemical separation. Applied Radiation and Isotopes, 2009, 67, 523-529.	0.7	26
43	Evaluation of [18F]gefitinib as a molecular imaging probe for the assessment of the epidermal growth factor receptor status in malignant tumors. European Journal of Nuclear Medicine and Molecular Imaging, 2008, 35, 1089-1099.	3.3	104
44	Synthesis and liposome encapsulation of a novel18F-conjugate ofω-conotoxin GVIA for the potential imaging ofN-type Ca2+ channels in the brain by positron emission tomography. Journal of Labelled Compounds and Radiopharmaceuticals, 2006, 49, 269-283.	0.5	13
45	Monitoring Tumor Glucose Utilization by Positron Emission Tomography for the Prediction of Treatment Response to Epidermal Growth Factor Receptor Kinase Inhibitors. Clinical Cancer Research, 2006, 12, 5659-5667.	3.2	199
46	Synthesis of an18F-fluorobenzoate idarubicin derivative as new potential PET radiotracer to predict chemotherapy resistance. Journal of Labelled Compounds and Radiopharmaceuticals, 2005, 48, 819-827.	0.5	7
47	Fluorine-18 labeling of 6,7-disubstituted anilinoquinazoline derivatives for positron emission tomography (PET) imaging of tyrosine kinase receptors: synthesis of18F-Iressa and related molecular probes. Journal of Labelled Compounds and Radiopharmaceuticals, 2005, 48, 829-843.	0.5	43
48	Impact on estrogen receptor binding and target tissue uptake of [18F]fluorine substitution at the 16I±-position of fulvestrant (faslodex; ICI 182,780). Nuclear Medicine and Biology, 2004, 31, 691-698.	0.3	28
49	Synthesis of 16α-fluoro ICI 182,780 derivatives: powerful antiestrogens to image estrogen receptor densities in breast cancer by positron emission tomography. Journal of the Chemical Society, Perkin Transactions 1, 2002, , 2275-2281.	1.3	16
50	18F-labeled difluoroestradiols: preparation and preclinical evaluation as estrogen receptor-binding radiopharmaceuticals. Steroids, 2002, 67, 765-775.	0.8	68
51	Synthesis of 2,16α- and 4,16α-difluoroestradiols and their 11β-methoxy derivatives as potential estrogen receptor-binding radiopharmaceuticals. Journal of the Chemical Society, Perkin Transactions 1, 2002, , 657-663.	1.3	26
52	Gamma radiation effects on potassium pertechnetate in carbonate media. Applied Radiation and Isotopes, 2001, 54, 45-51.	0.7	13
53	Synthesis of 2, 16α―and 4, 16αâ€{16αâ€< sup>18F]difluoroestradiols and their 11βâ€methoxy derivat estrogen receptor imaging. Journal of Labelled Compounds and Radiopharmaceuticals, 2001, 44, S348.	ives for	3